DIAGNOSTYKA 2016, Vol. 17, No. 4

ISSN 1641-6414
e-ISSN 2449-5220

APPLICATION OF THE TEAGER-KAISER ENERGY OPERATOR TO DETECT INSTABILITY OF A PLAIN BEARING

Jędrzej BLAUT, Tomasz KORBIEL, Wojciech BATKO
AGH University of Science and Technology, blaut@agh.edu.pl

Summary

The paper presents application of a non-linear method (energy operator) to monitor the operation of a plain bearing. The possibility of using the energy operator to evaluate the energy of a simulated mechanical system was analysed. Then, an experiment was conducted in the laboratory environment which involved observation of oil vortexes. This allowed to show the possibility of using the energy operator as a descriptor of operating state of a hydrodynamic bearing.

Keywords: Kaiser, Teager, TKEO, energy operator, hydrodynamic lubrication, fluid bearings, dynamic stability, nonlinear analysis

ZASTOSOWANIE OPERATORA ENERGETYCZNEGO TEAGER-KAISERA DO DETEKCJI NIESTABILNOŚCI ŁOŻYSKA ŚLIZGOWEGO

Streszczenie

W artykule zaprezentowano użycie metody analizy nieliniowej jaką jest operator energetyczny w celu monitorowania pracy łożyska ślizgowego. Przeanalizowano możliwość użycia operatora energetycznego w celu oceny energii symulowanego układu mechanicznego. Potwierdziło to zależność pomiędzy energią w ujęciu newtonowski a wartością operatora energetycznego. Następnie przeprowadzono eksperyment na stanowisku laboratoryjnym polegający na obserwowaniu powstawania drgań olejowych. Pozwoliło to wskazać na możliwość stosowania operatora energetycznego jako deskryptora stanu pracy łożyska hydrodynamicznego.

Słowa kluczowe: Kaiser, Teager, TKEO, operator energetyczny, smarowanie hydrodynamiczne, łożyska ślizgowe, stabilność, analiza nieliniowa

1. DIAGNOSTICS OF NON-LINEAR SYSTEMS

Diagnostics of technical systems requires an analysis of non-linear issues. Although many machines can be described with a linear model, non-linear disturbance can occur during their operation. Such disturbance can be caused by wear or a variable character of operation. There are however many objects which cannot be correctly described with a linear model. One of them is a hydrodynamic bearing. Despite a lot of research in many scientific centres, the complexity of physical phenomena occurring in a hydrodynamic bearing causes an unceasing interest of the researchers. The proposed mathematical models of hydrodynamic bearings allow to accurately foresee their operation, but many parameters have to be determined and entered. The development of parameters and the simulation itself are time-consuming [1]. The diversity of bearing designs results in development of new numerical models [2,3]. Use of water as a lubricant allows to observe the complexity of impact of water technological parameters on the stable operation of the bearing. The operation of a hydrodynamic bearing can also be disturbed by oil vortexes the development physics of which has not been identified sufficiently [4]. As the simulations of operation of hydrodynamic bearings are complex and time-consuming, it is necessary to search for effective methods to analyse diagnostic signals based on non-linear analysis. New lubricants are additional difficulty in the analysis of the hydrodynamic bearing behaviour. Due to environmental considerations, there is an increasing requirement to use lubricants which are not hazardous in case of an accidental release to the environment. Difficult control of technological parameters of, for example, water causes unpredictable changes of lubricant film thickness [5].

The paper compares the similarities of energy operator to total energy of an object in order to check the possibility of using the energy operator as a descriptor of correct bearing operation. The considerations are theoretical, and in the final part they were verified on a dedicated laboratory test stand.

2. ENERGY OPERATOR

The energy operator was introduced in 1983 in a paper by Hubert M. Teager and Shushan M. Teager [6]. The authors emphasized a few applications of the

operator (including speech analysis), but did not explain the theory. The paper by J. F. Kaiser [7] introduced an algorithm to calculate the energy operator and gave theoretical background for a continuous signal and a discrete form for a periodic signal. Currently the Teager-Kaiser operator, also called the Kaiser operator, has a wide application[13,14].

The energy operator was successfully used in research on a helicopter bearing [8]. An important advantage of the method was ability to operate on raw signal which allowed to analyse the whole frequency band without the need of band-pass filtration. The interest in the energy operator in diagnostics is also noted in research on gearboxes used in wind turbines [9]. The gearbox operates in conditions of varying load and temperature. The research showed that the diagnostics technique using the energy operator is as effective as the traditional technique based on Hilbert transform.

There are many ways to give a definition of the energy operator. The aforementioned paper by the Teagers presented only the diagrams of the operator. The energy operator can be compared to total energy of an object in the Newtonian sense. It is a sum of potential and kinetic energy of an object. Further in the paper a relationship is presented between the energy operator and the basic mechanical models, including the bearing model. In case of a simple system with single degree of freedom, the total mechanical energy is the sum:

$$E = \frac{1}{2}kx^2 + \frac{1}{2}mv^2 \tag{2.1}$$

where E is total energy, k – stiffness coefficient, x – displacement, m – mass, v – velocity.

Examining the energy of natural vibration of a system with single degree of freedom which equation of motion is

$$m\,\ddot{x} + kx = 0 \tag{2.2}$$

where $\ddot{x}$ is the second derivative of displacement- acceleration. The solution is the function

$$x = A\cos(\omega t + \varphi) \tag{2.3}$$

where A is amplitude, $\omega=\sqrt{(k/m)}$ – frequency, t – time, φ – any phase. The total mechanical energy of the system according to (2.1) is equal to:

$$E = \frac{1}{2}m\omega^2 A^2 \tag{2.4}$$

Equation 2.3 indicates that the object energy is proportional to the half of the quotient of amplitude squared and the angular frequency squared.

The energy operator is defined in the continuous form as [5,7]:

$$\Psi(x(t)) = \dot{x}^2(t) - x(t)\ddot{x}(t) \tag{2.5}$$

Where $\dot{x}$ is the derivative of displacement- velocity which for systems with single degree of freedom, and thus for sinusoidal signal x(t)=Acos(ωt), takes the form:

$$\Psi(x(t)) = (-A\omega\sin(\omega t))^2 - A\cos(\omega t)(-\omega^2 A\cos(\omega t)) = \tag{2.6}$$

$$= A^2\omega^2(\sin^2(\omega t) + \cos^2(\omega t)) = \tag{2.7}$$

$$= A^2\omega^2 \tag{2.8}$$

Comparing the relationships 2.4 and 2.8 one can see the similarity of energy operator to the total energy of an object in the Newtonian sense for a simple system described by the equation of motion 2.2. Both relationships are a function of the quotient of amplitude and frequency squared. In addition, the energy equation 2.4 depends on elasticity constant which is invariable for majority of systems.

2.1. Natural vibration of a system with single degree of freedom

When we consider a system with single degree of freedom described by the equation of motion 2.2, we obtain the solution 2.3. Figure 1 presents the waveform of displacement, energy and energy operator for a naturally vibrating system with single degree of freedom for parameters: m=1, k=1. In line with expectations, the system with constant energy has a constant value of energy and energy operator during the simulation.

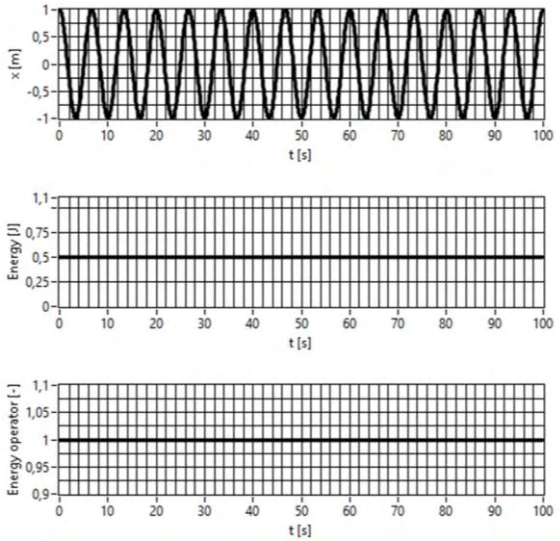

Fig. 1. Diagrams of displacement, energy and energy operator for a naturally vibrating system with single degree of freedom for parameters: m=1, k=1, initial conditions: x=1, $\dot{x}$=0

A discrete form of the energy operator can be derived for many systems. For example for the system described by equation 2.2, the energy operator can take a discrete form:

$$\Psi[x[n]] = x^2_{[n]} - x_{[n-1]}x_{[n+1]} \tag{2.9}$$

assuming that the signal is periodic:

$$x_n = A\cos(\Omega n + \varphi). \tag{2.10}$$

then:

$$x_n = A\cos(\Omega n + \varphi). \tag{2.11}$$

$$x_{n-1} = A\cos(\Omega(n-1) + \varphi) \tag{2.12}$$

$$x_{n+1} = A\cos(\Omega(n+1) + \varphi) \tag{2.13}$$

Where $\Omega = 2\pi f/Fs$, and Fs sampling frequency. From trigonometrical identities:

$$\cos(\alpha+\beta)\cos(\alpha-\beta) = \frac{1}{2}[\cos(2\alpha) + \cos(2\beta)] \tag{2.14}$$

$$\cos(2\alpha) = 2\cos^2(\alpha) - 1 = 1 - 2\sin^2(\alpha) \tag{2.15}$$

we obtain equality:

$$x_{n-1}x_{n+1} = A^2\cos^2(\Omega n + \varphi) - A^2\sin^2(\Omega) \tag{2.16}$$

substituting to equation 2.9 we obtain:

$$x^2_n - x_{n-1}x_{n+1} = A^2 \sin^2(\Omega) \qquad (2.17)$$

This relationship is correct assuming that Ω is positive and less than π/2. In practical applications, Ω cannot exceed ¼ of sampling frequency. Relationship 2.17 can be approximated also for small values of Ω so that sin(Ω) = Ω. For Ω< π/2 the approximation error does not exceed 11.2%. The advantage of discrete form is ability to track the energy operator on a current basis using a small computational capacity [10].

2.2. Energy operator for damped vibration

While analysing the behaviour of energy operator for damped systems we used a model of a system with natural vibration damped linearly

$$m\ddot{x} + c\dot{x} + kx = 0 \qquad 2.18$$

and natural vibration damped non-linearly which is a simple model of plain bearing:

$$\ddot{x} + \omega^2 x - 2h\dot{x} - \beta\dot{x}^3 = 0 \qquad 2.19$$

where h,c – parameters related to damping coefficient: $\frac{c}{m}$=2h, β – parameter related to damping coefficient. For naturally damped vibration described by equation of motion 2.18 the solution can be described by equation:

$$x(t) = Ae^{-ht}\cos((\lambda t + \Phi) \qquad 2.20$$

where λ – vibration type parameter, $\lambda^2 = \omega^2 - h^2$. It is a solution of equation 2.18 for a subcritical dampening. For solution 2.19, energy according to formula 1.1 is:

$$E = \frac{1}{2}A^2\left(e^{-ht}\right)^2 (\cos(\lambda t + \Phi)^2 h^2 m + 2h\lambda m \cos(\lambda t + \Phi)\sin(\lambda t + \Phi) + \sin(\lambda t + \Phi)^2 \lambda^2 m + k\cos(\lambda t + \Phi)^2) \qquad 2.21$$

The energy operator according to formula 2.4 takes the form:

$$\Psi(x(t)) = A^2(e^{-ht})^2\lambda^2(\cos(\lambda t + \Phi)^2 + \sin(\lambda t + \Phi)^2) = A^2\left(e^{-ht}\right)^2\lambda^2 \qquad 2.22$$

The behaviour of such system was analysed. Figure 2 presents the equation of motion of the system, its energy and energy operator for parameters: m=2, k=4, c=1. Analysing the behaviour of the system, we can see that the vibration amplitude constantly decreases. In the energy vs. time diagram we can see the change of energy dissipation during motion. When the velocity is zero according to equation 2.18, the energy is constant. The diagram of energy operator defined by formula 2.22 has a similar character to the function of amplitude drop Ae^{-ht}.

The character of non-linear vibration described by equation of motion 2.19 for parameters m=3, k=3, c=1, $\beta = 1$ is presented in Figure 3. Parameter β impacts the oscillation amplitude; when $\beta = 0$ we obtain the equation for a system with vibration dampened linearly. When $\beta > 0$ the vibration decay quicker, when $\beta < 0$ the vibration decay slower.

Application of the operator allows to observe one parameter representing displacement, velocity or acceleration which can be essential in detection of formation of a hydrodynamic instability in the bearing. Exceeding the displacement limit value can mean self-excited vibration, and increase of acceleration or velocity can mean occurrence of oil vortexes.

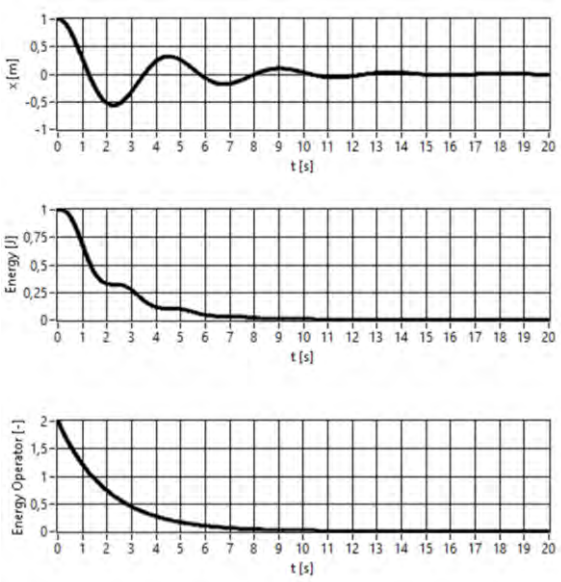

Fig. 2. Diagrams of displacement, energy and energy operator for a vibrating system with linear dampening, with single degree of freedom, described by equation 2.18 for parameters: m=2, k=4, c=1, initial conditions: x=1, $\dot{x}$=0

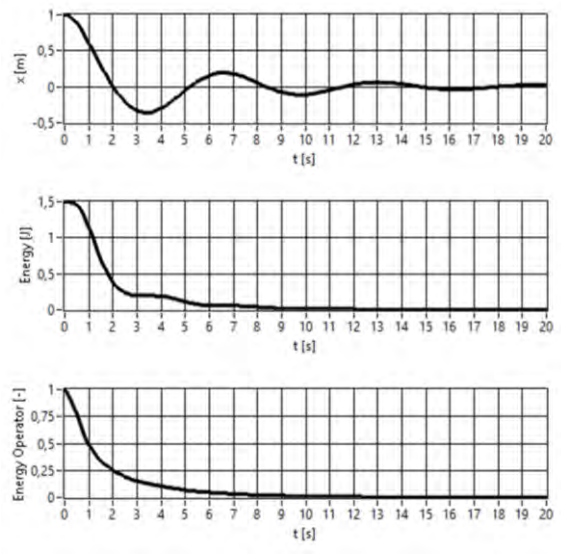

Fig. 3. Diagrams of displacement, energy and energy operator for a vibrating system with non-linear dampening, with single degree of freedom, described by equation 2.19 for parameters m=3, k=3, c=1, $\boldsymbol{\beta = 1}$, initial conditions: x=1, $\dot{x}$=0

3. TESTS

Tests were conducted in order to verify the effectiveness of using the Teager-Kaiser energy operator in the diagnostics of hydrodynamic states of a plain bearing. The inference was conducted on the basis of results of experiments on a simulated and a

real object. The correct operation and occurrence of oil vortexes was recorded on the real object. This allowed to determine the value of energy operator depending on the hydrodynamic state of the bearing.

3.1. Simulation tests of a non-linear object

The simulation tests were performed in order to determine the possibility of applying the energy operator to diagnose the hydrodynamic state of the plain bearing. The following equation was used:

$$\ddot{x}+kx+2h\dot{x}-\beta\dot{x}^3=0,\ k>0,\ 2h>0,\ \beta>0 \qquad 3.1$$

where $2h, \beta$ – parameters related to damping coefficient, k – stiffness coefficient, x – displacement. The equation 3.1 was taken from literature [11]. It allows to describe the behaviour of a non-linear object and it can model the dampening which occurs in plain bearings. The stability of the system was considered in the Lyapunovian sense in order to analyse the system behaviour. The system 3.1 has three singularities (0,0), $(-\sqrt{\frac{k}{2h}},0)$, $(\sqrt{\frac{k}{2h}},0)$. The first of them is stable, and the remaining two are unstable. The diagram of phase trajectories with marked singularities is presented in Figure 4. It illustrates all possible states of the system. The system can feature instability which tries to increase the displacement and velocity (quadrant II) or instability which reduces the displacement and velocity (quadrant III). It is important for the research because the energy coefficient defined as a difference of velocity squared and the quotient of displacement and acceleration (equation 2.5) is sensitive to the change of sign. The change of positive value of position or acceleration to negative can cause an abrupt increase of the energy coefficient. The energy coefficient can be negative when the value of quotient of displacement and acceleration is greater than the value of velocity. The change of sign can cause difficulties in an unambiguous evaluation of the change of energy operator.

In order to test the possibility of applying the energy operator as an instability predictor, the coefficients were chosen in such a manner as to make the instability develop in two possible directions. The first instability development option was analysed for the system described by equation 3.1 with parameters 2h=0.2, β=0.274, k=1, m=1. The second instability development option was analysed for the system described by equation 3.1 with parameters 2h=0.2, β=0.28, k=1, m=1. The phase trajectory diagram was plotted and the system analysis was carried out until the root of sum of squares exceeded value 5 in order to show the occurrence of instability.

When the limit of velocity limit value is exceeded, a dangerous state occurs which can lead to the bearing failure. The displacement, energy, and the Teager-Kaiser energy operator waveforms are presented in Figures 6 and 7. In both cases the sign of energy operator changes from positive to negative. This results from a sharp increase of acceleration absolute value which is included in the definition of energy operator. This is related to the simulation conditions; the equation is solved until the instability increases significantly. Occurrence of instability can be however unambiguously detected before the energy operator sign changes. The instability occurring in Figures 6 and 7 can be seen in the energy diagram and the energy operator diagram before the sign changes. It is characterized by amplitude increasing a few times. The displacement diagram does not allow to detect instability.

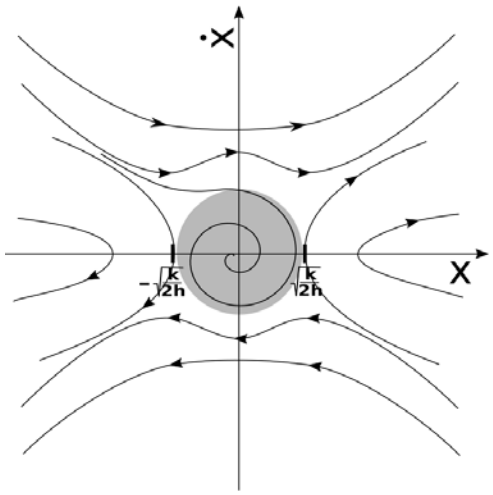

Fig. 4. Phase trajectory for the system described by equation 3.1. The shaded area represents local stability

The simulation instability tests indicate that the Teager-Kaiser energy operator responds before the phase trajectory goes beyond the stable operation area. This allows to detection a hydrodynamic instability before it occurs, and this it gives more time to react and prevent the occurrence. **The advantage of the energy operator analysis over the system energy analysis is that the former does not require the knowledge of the system parameters such as dampening, elasticity and mass.**

The tests stand presented in Figure 8 comprises a motor with speed control. The motor is connected via a coupling to a shaft with rolling bearings on both ends. In the middle of the shaft is the tested plain bearing with two eddy-current sensors. These sensors detect distance which allows to directly plot shaft axis trajectory (orbit, shaft centre trajectory). The laser tachometer measures the shaft rotational speed. The lubricant is delivered to the bearing from the tank and is returned there; it is a closed lubricant circuit. The signal from the tachometer and eddy-current sensors is recorded by means of a measurement card with the 4200 Hz sampling frequency. The recorded data are analysed in proprietary software which allows to remove the runout phenomenon, plot the shaft axis trajectory, and determine the value of the Teager-Kaiser energy operator according to formula 2.5.

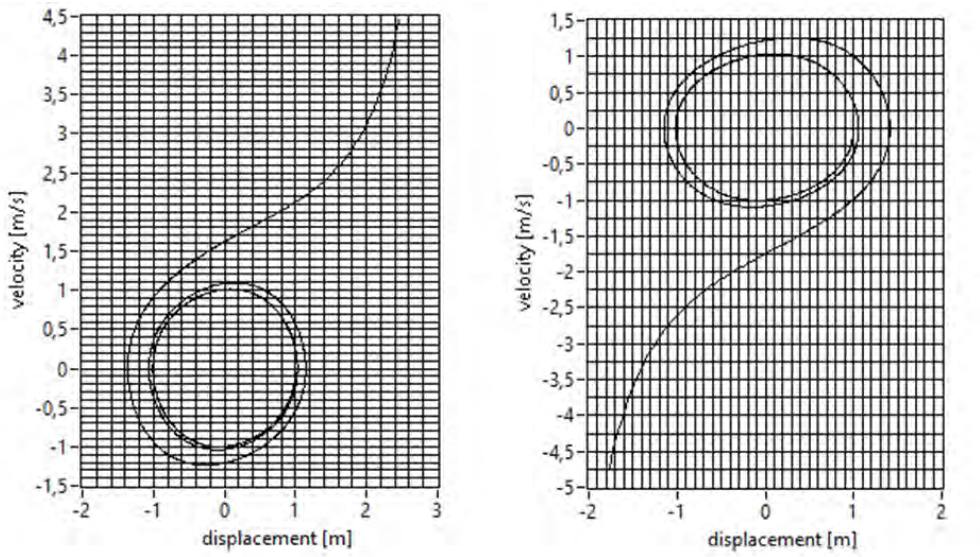

Fig. 5. Phase trajectories for vibration of systems with single degree of freedom described by equation 3.1; left-hand diagram: 2h=0.2, β =0.274, k=1, m=1, initial conditions: x=1, $\dot{x}$ =0; right-hand diagram: 2h=0.2, β =0.28, k=1, m=1 initial conditions: x=1, $\dot{x}$ =0

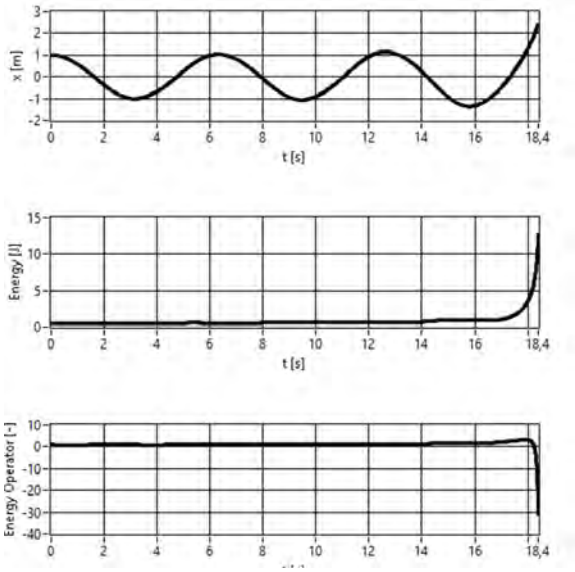

Fig. 6. Diagrams of displacement, energy and energy operator for a system with single degree of freedom described by equation 3.1 for: 2h=0.2, β =0.274, k=1, m=1, initial conditions: x=1, $\dot{x}$ =0

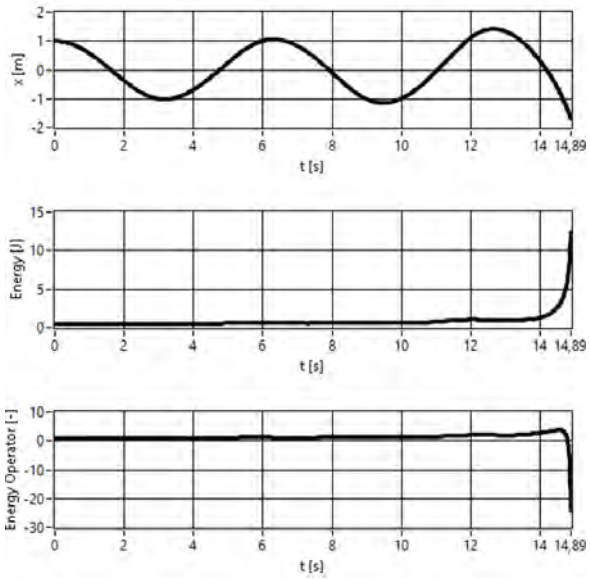

Fig. 7. Diagrams of displacement, energy and energy operator for a system with single degree of freedom described by equation 3.1 for: 2h=0.2, β =0.28, k=1, m=1, initial conditions: x=1, $\dot{x}$ =0

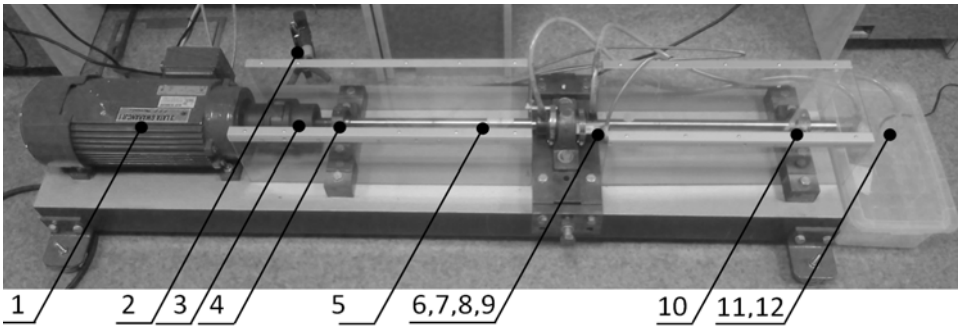

Fig. 8. Test stand, 1- motor with speed control, 2-tachometer, 3-coupling, 4,10- rolling bearing, 5-shaft, 6-plain bearing, 7-bearing loading system, 8-lubricant delivery and removal valves, 9- eddy-current sensors, 12- lubricant tank

3.2. Experiments on laboratory test stand

During the experiment the stand was loaded with the force of 140 N in the horizontal plane by the bearing loading system (6). This corresponds to the shaft deflection by 1mm. The lubricant was water; this required a bearing adapted to water lubrication. The choice was a bearing with rubber lining and longitudinal grooves.

The experiment involved examining the trajectory of shaft rotation axis. The experiment was conducted at various speeds, from 300 to 6800 RPM, in 500 RPM increments. The recorded signal was analysed, allowing to diagnose the individual hydrodynamic states during the bearing operation.

3.3. Identification of hydrodynamic states

According to the literature [12], there are three hydrodynamic states in plain bearings: normal operation, small oil vortexes, large oil vortexes. These trajectories are plotted on the basis of two revolutions; 0° means the beginning of observation, 360° is the shaft axis position after the first revolution, 720° is the shaft axis position after the second revolution. During normal operation there is one phase marker: 0° = 360° = 720°. There are two phase markers for small oil vortexes, and three for large oil vortexes.

The purpose of measurements analysis was to find a method to detect a hydrodynamic instability. The reference was the diagram of trajectory of shaft rotation axis for two revolutions as a predictor of hydrodynamic state.

Figures 10 and 11 present examples of trajectory diagrams obtained on the test stand in successive hydrodynamic states. The diagrams were plotted on the basis of measurements made on the stand at 5000 RPM and 140 N load force.

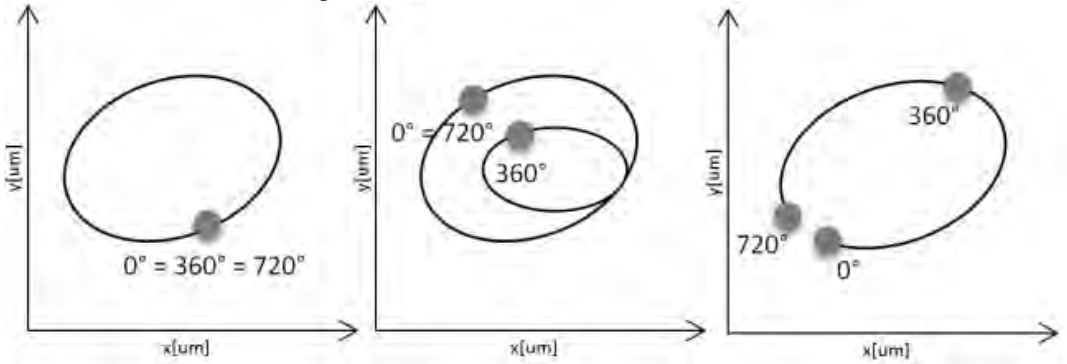

Fig. 9. Phase markers (0°start of revolutions, 360° one full revolution, 720° two full revolutions) as a diagnostic indicator of the bearing hydrodynamic state. I normal operation area, II area of small oil vortexes, III area of large oil vortexes

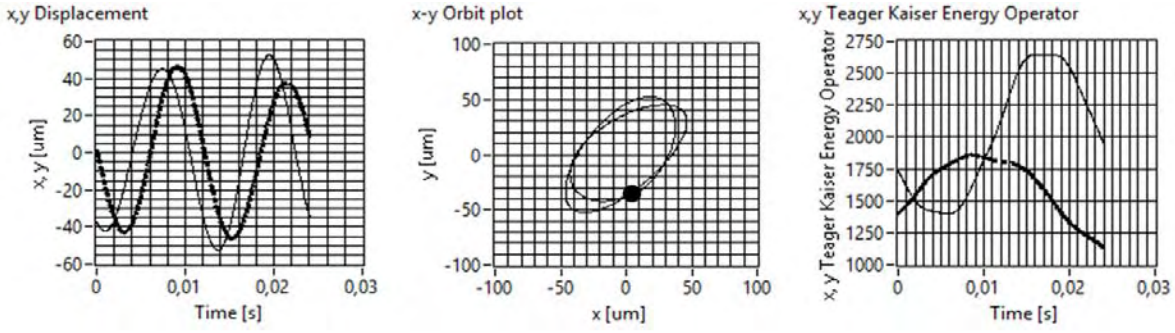

Fig. 10. Displacement [um], orbit [um], and energy operators in two axes (x and y). Operating parameters: 5000 RPM, 140 N load, lubricant: water. Stable trajectory; energy operator mean value: 2000 and 1600 (for axes x and y); energy operator amplitude: 1300 and 800 (for x and y)

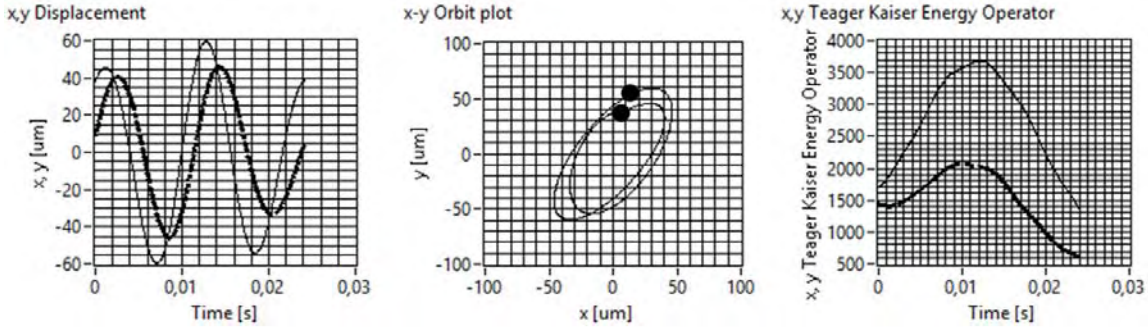

Fig. 11. Displacement [um], orbit [um], and energy operators in two axes (x and y). Operating parameters: 5000 RPM, 140 N load, lubricant: water. Unstable trajectory, area of area of small oil vortexes; energy operator mean value: 2750 and 1520 (for axes x and y); energy operator amplitude: 2330 and 1400 (for x and y)

The diagrams shown in Figures 10 and 11 present two hydrodynamic states (normal operation and small oil vortexes) of the bearing operation for the same operating parameters. The energy operator diagram shows a significant increase of vibration amplitude. This allows to say that monitoring the energy operator amplitude can be used to detect the hydrodynamic instability occurring in bearings. Unlike the simulations, the tests on the real objects allowed to see a problem relating to the energy operator oscillation. The amplitude and mean were used to describe the energy operator behaviour.

4. CONCLUSION

The paper consists of three parts: analytical, simulation and experimental on the laboratory test stand. Observation of energy operator behaviour during the simulation and the experiment indicated a **significant increase of the energy operator amplitude in case of occurrence of small oil vortexes.** The oil vortexes were identified by means of phase markers on the trajectory diagram. The trajectory corresponding to oil vortexes has a different signal variability dynamics which is a direct cause of increased energy operator amplitude.

An experiment was also conducted which involved observation of large oil vortexes. When the load was intentionally reduced, there was a dangerous state of large-amplitude shaft vibration, typical for bearings under a low load. Although such vibration did not result in a change of trajectory or increase of the number of phase markers, it significantly **increased the energy operator mean value** which can be linked with the diameter of trajectory of the centre of shaft rotation axis. The increased energy operator amplitude in this case is directly related to the reduction of lubricant film thickness which increases the shaft displacement.

REFERENCES

1. Boyaci A. Procedia IUTAM. Numerical continuation applied to nonlinear rotor dynamics. 2016: 255 – 265.
2. Batko W, Kiciński J, Dąbrowski Z. Nonlinear effects in technical diagnostics. Radom: PAN Polish Academy of Sciences, 2008.
3. Pai RS, Pai R. Stability of four-axial and six-axial grooved water-lubricated journal bearings under dynamic load. Mechanical Engineering. 2008; 222(5): 683-691.
4. Kiciński J, Żywica G. Numerical analysis of defects in the rotor supporting structure. Adv. Vib. Eng. 2012; 11 (4): 297-304.
5. Korbiel T, Blaut J, Uliński A. The characteristics of Iubricants of hydrodynamic bearings on selected technological water parameters. Przegląd Mechaniczny 2015; 4:36-39.
6. Teager H, Teager S. A Phenomenological model for vowel production in the Vocal Tract. San Diego 1983: College-Hill Press.
7. Kaiser J. On a Simple Algorithm to Calculate the 'energy' of a Signal. IEEE Proc. ICASSP-90. 1990.
8. Henríquez P. Application of Teager-Kaiser energy operator to the analysis of degradation of a helicopter input pinion bearing. The International Conference Surveillance 6. 2011.
9. Antoniadou I. A time–frequency analysis approach for condition monitoring of a wind turbine gearbox under varying load conditions. Mechanical Systems and Signal Processing 2015:188–216.
10. Kvedalen E. Signal processing using the Teager Energy Operator and other nonlinear operators. Cand. Scient Thesis. 2003.
11. Bogusz W. Stateczność Techniczna. Warszawa: IPPT PAN, PWN, 1972.
12. Kiciński J. System oceny stanu dynamicznego maszyn wirnikowych. Dynamika wirników i łożysk ślizgowych. Gdańsk: Szewalski Institute of Fluide-Flow Machinery, 2005: 321-326.
13. Li H, Fu L, Zhang Y. Bearing faults diagnosis based on teager energy operator demodulation technique. Measuring Technology and Mechatronics Automation, 2009; 1:594-597.
14. Gałęzia A. Averaged signal measures of TKEO energy waveform in detection of tooth break in gearbox. Pomiary Automatyka Kontrola, 2014; 60:31-34.

Received 2016-06-22
Accepted 2016-10-14
Available online 2016-11-21

Jędrzej BLAUT MSc, is a PhD student at the Department of Mechanics and Vibroacoustics of the Kraków University of Technology. His interests are related to technical diagnostics, signals analysis and modern measurement systems.

Tomasz KORBIEL PhD, Eng. is an assistant professor in the Department of Mechanics and Vibroacoustics, AGH. His interests are related to the diagnosis technical and systems monitoring in the technique